Mechanics of energy harvesters based on tensegrity solar facades

IOP Conf. Series: Materials Science and Engineering **999** (2020) 012003 doi:10.1088/1757-899X/999/1/012003

Mechanics of energy harvesters based on tensegrity solar facades

R Miranda[1], E Babilio[2], N Singh[1], D P Villamil[1], F Santos[3], F Fraternali[1]

[1] Department of Civil Engineering, University of Salerno, Salerno 84084, Italy
[2] Department of Structures for Engineering and Architecture (DiSt), University of Naples "Federico II", Naples 80134, Italy
[3] FCT, Civil Engineering Department, Universidade NOVA de Lisboa, 2829-516 Caparica, Portugal
Email: ramiranda@unisa.it; enrico.babilio@unina.it; snarinder@unisa.it; dianamaritzap@gmail.com; fpas@fct.unl.pt; f.fraternali@unisa.it

Abstract. This work is focused on the computational design of tensegrity shading systems of energy efficient buildings which mitigate air conditioning consumption and optimize the energy performance of the building. It is concerned with the design of active solar façade screens based on lightweight tensegrity units, which are easily integrated with energy harvesting piezoelectric cables. The unit cells of the analyzed screens are controlled by tensioning and releasing selected cables of the structure and are used to direct the shading panels towards the sun. A numerical procedure simulates the dynamics of the analyzed tensegrity façades, by considering the opening and closure motions of the screens, and the vibrations produced by the action of dynamic wind forces. The energy harvesting ability of the proposed façade is numerically estimated.

1 Introduction

The design of sustainable buildings naturally leads to analyze the fundamental elements of such buildings, which consist of mechanical ventilation systems, protective shading systems, and, eventually, home automation systems and renewable energy harvesting devices. Reduction of energy consumption and carbon dioxide emissions through intelligent and sustainable systems is one of the key objectives of EU's Horizon 2020 program "SC3" [1]. The demand for energy savings and the excessive CO_2 emissions generated by buildings has called for the use of new "interactive building envelopes", defined as systems that interacts with the variations of the external climatic conditions by means of automatic control devices, optimizing the environmental performance of the internal microclimate. This paper presents a mechanical study of dynamic sunscreens with tensegrity systems for the re-designing of the Al Bahar Towers facade in Abu Dhabi [2]-[4]. We enrich the kinematical study presented in [2] by providing an analytical procedure for the implementation of the system and the dynamics under wind forces. We employ such a procedure for the simulation of the motion exhibited by origami sunscreens under fluctuating (positive/negative) wind forces. The wind-induced energy stored in the activation strings is investigated with the aim of exploring the potential of the analyzed sunscreens as wind power harvesters. Their energy harvesting capacity is compared with that of microeolic turbines available in the market [5]-[7]. The results show that tensegrity solar façades as wind power harvesters are highly feasible, and may lead to design of cost-effective shading systems, which are energetically autonomous and do not require power from the electric grid for their operation.

2 WTABS Model

In the present study a tensegrity module, addressed as 'wind tensegrity Al Bahar screen' (WTABS), is analyzed in order to evaluate its ability in harvesting wind energy [8]. In order to harvest mechanical energy, the TABS module is enhanced with a number of D-bars equipped with strings wrapped by PVDF piezoelectric films as shown in Figure 1, which describes the full WTABS model. The actuation mechanism is generated by a piston Rolaram® R2501190, with design characteristics of dynamic loading equal to 294 kN and a maximum stroke of 3500 mm [9], which is located on the highest point of the WTABS structure. Such a piston stretches and releases the perimetric strings, thus activating the dynamic motion. A telescopic sliding constraint positioned behind the structure adjusts the scrolling along the z axis, while two linear springs with stiffness constant K = 67 kN m^{-1} control the movements in-plane of the other vertices.

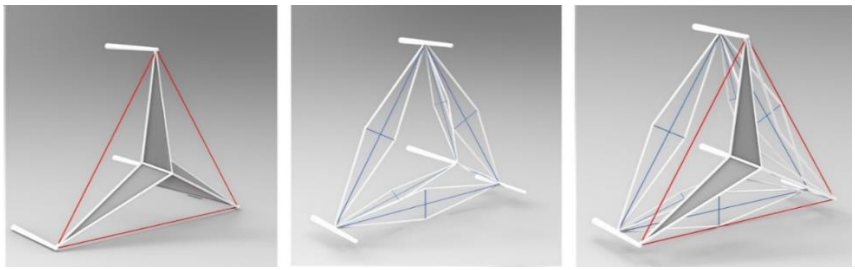

Figure 1. (a) TABS configuration; (b) D-bar elements; (c) construction of the WTABS system.

3 Computational modeling of the WTABS dynamics

In this section, we describe an algorithm for the rigid body dynamics, in matrix form, that includes the cable masses and bar length constraints and handles a rigidity constraint on the deformation of the bars. We will indicate matrices with bold capital letters (i.e. **X**), diagonal matrices with letters with a superimposed hat (i.e. $\hat{x}$), vectors with bold lower-case letters (i.e. **x**), and scalars with italic letters (i.e. *x*).

For this purpose, we consider a general tensegrity network made of n_n nodes, n_b bars and n_s strings. By introducing the force densities parameter of the k^{th} cable as:

$$\gamma_k = \max\left[0, k_k\left(1-\frac{L_k}{s_k}\right)\right]+\gamma_{ck}, \text{ where } \begin{array}{ll} \gamma_{ck} = c_k\dot{s}_k/s_k & if:\ s_k \geq L_k, \\ \gamma_{ck} = 0, & if:\ s_k < L_k. \end{array} \tag{1}$$

being γ_{ck} the force density due to damping, we can write the equations of motion of a class 1 tensegrity system as follows [10]:

$$\ddot{\mathbf{N}}\mathbf{M} + \mathbf{N}\mathbf{K} = \mathbf{W} \tag{2}$$

where **M** and **K** are respectively the mass matrix and the stiffness matrix defined as

$$\mathbf{M} = \frac{1}{12}\mathbf{C}_\mathbf{B}^T\hat{m}\mathbf{C}_\mathbf{B} + \mathbf{C}_\mathbf{R}^T\hat{m}\mathbf{C}_\mathbf{R}\,, \qquad \mathbf{K} = \mathbf{C}_\mathbf{S}^T\hat{\gamma}\mathbf{C}_\mathbf{s} - \mathbf{C}_\mathbf{B}^T\hat{\lambda}\,\mathbf{C}_\mathbf{B} \tag{3}$$

Here $\mathbf{C_B}$, $\mathbf{C_S}$ and $\mathbf{C_R}$ are the connectivity matrices of bars, cables and centers of mass and λ represent the force density in bars per unit length:

$$-\hat{\lambda} = \frac{1}{12}\left[\dot{\mathbf{B}}^T\dot{\mathbf{B}}\right]\hat{m}\,\hat{l}^{-2} + \frac{1}{2}\left[\mathbf{B}^T(\mathbf{W}-\mathbf{S}\hat{\gamma}\mathbf{C_s})\mathbf{C}_\mathbf{B}^T\right]\hat{l}^{-2} \tag{4}$$

where $\hat{l}^{-2}$ is a diagonal matrix of terms $l_k^{-2} = \|\mathbf{b}_k\|^{-2}$ (see [8] for further details).

In the field of form finding tensegrity methods, the force density method is used to convert the nonlinear equilibrium systems into linear ones through the transformation between force density (the control variable that appears linearly in the system) and rest length. We apply fourth-order Runge-Kutta method to integrate equation (2) [11]-[13].

4 Numerical applications

The dynamics of the system and the corresponding amount of convertible mechanical energy are investigated under two basic processes, namely motion driven by ram activation and wind fluctuations, due to wind gusts loading the deployed screen by considering the damping factor of 5%, a time step of 0.025 s.

4.1 Simulation of the activation motion of the WTABS module

In this section we assume that the screen is activated by a force acting on a node, that we call as the *actuated node*, impressed by the linear actuator. The loading program, divided in two phases of 40 seconds each, consists in deploying the screen from the initial state to the almost flat configuration, by linearly increasing over time the actuating force, and then maintaining the screen deployed, with the force held constant over time. At t=0 s, the force on the actuated node has value $F_{\min}$=72.690 kN, necessary to sustain the initially pre-stressed configuration. At t=20 s, the external force reaches its maximum value, set to $F_{\max}$=276.221 kN. Notice that, in order to save energy in an actual application, when the screen is folded or deployed at the desired configuration, the actuated node could be locked with a releasable hook and the actuator could be switched off. Whenever the screen configuration must be changed, actuator could be switched on and the hook released. The initial configuration of the system corresponds to the screen almost folded, with initial velocities set to zero. In the chosen initial state, boundary strings are under tensile stress, which is computed as:

$$N_0 = \frac{E_S A_S}{L_0}(L_i - L_0) = 11846.6 \text{ N} \tag{5}$$

where E_s and $A_s = \pi\,(d/2)^2$ are effective Young's modulus and cross-sectional area of the string and L_0 and L_i are rest and initial lengths, respectively given by:

$$L_0 = \frac{\sqrt{2}}{2}L = 3.94042 \text{ m} \qquad \text{and} \qquad L_i = 4.09281 \text{ m} \tag{6}$$

Notice that the rest length is equal to the distance of the boundary nodes of the screen in its fully folded state, which is a purely theoretical and not achievable configuration. This, indeed, ensures that boundary strings in actual applications cannot be stress-free. In Figure 2, the solution is reported with respect to three deformed configurations, namely the initial state, an intermediate level of unfolding, at t = 25 s, and the deployed configuration.

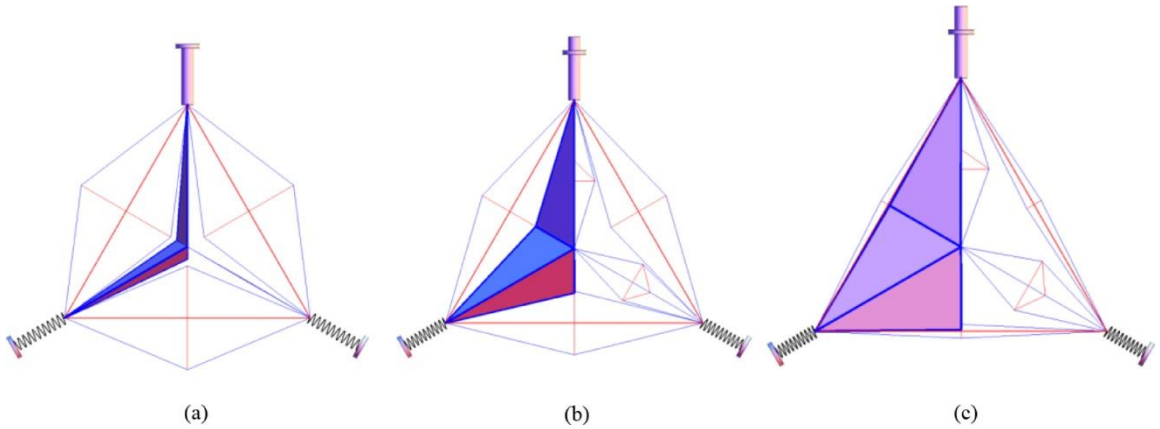

Figure 2. Three configuration of screen and underlying assemblage of D-bars: at t = 0 s (a), t = 25 s (b), and t = 50 s (c). The boundary springs and the actuator ram are represented with amplified scales.

4.2 Modeling of the wind forces

The instantaneous wind vector speed **V**(P,t) can be represented by the sum of the average speed $\mathbf{V}_m$(P) over an interval of 10 min, characterized by long-term variations, and the atmospheric turbulence **V′**(P,t), with high frequency fluctuations [14]:

$$\mathbf{V}_m(P) = \mathbf{i} \cdot v_m(z) \tag{7}$$

$$\mathbf{V}'(P,t) = \mathbf{i} \cdot v'_1(P,t) + \mathbf{j} \cdot v'_2(P,t) + \mathbf{k} \cdot v'_3(P,t) \tag{8}$$

where P is any point at the altitude z on the ground, t is the time, **i**, **j**, **k** are the unit vectors along axes x, y, z; v_m is the average speed along x and v'_1, v'_2, v'_3 are the longitudinal (x), lateral (y) and vertical (z) component of turbulence. We consider only the value of v'_1 (v' from now on) specified by the spectral density [14]:

$$S_L(z,n) = \frac{6.8\, f_L(z,n)}{(1 + 10.2\, f_L(z,n))^{5/3}} \tag{9}$$

where $f_L(z,n)$ is a dimensionless frequency

$$f_L(z,n) = \frac{nL(z)}{v_m(z)} \tag{10}$$

being $L(z)$ the turbolence scale and n the natural frequency.

By selecting a frequency step Δn=0.05 Hz, and a set of 100 frequencies n_k=(k-1/2) Δn, k=1,…,100, we generate a sample of the variable wind speed using the superimposition method with sinusoidal functions, that is [15]:

$$v'(z,t) = \sum_{k=1}^{N} \sqrt{2\, S_L(z,n_k)\Delta n}\, \cos(2\pi n_k t + \varphi_k) \tag{11}$$

with φ_k randomly generated phase angles over the range 0-2π. Finally, the peak value of the wind kinetic pressure, in m/s, is expressed by:

$$q_p(z,t) = \frac{1}{2}\rho\big(v_m(z) + v'(z,t)\big)^2 \tag{12}$$

being ρ=1.25 kg m^{-3} the density of the air.

For the sake of computation, we assume data are compatible with Al Bahar Towers, that is height z*=120 m in a caostal area exposed to wind, leading to the turbolence scale $L(z^*)$=40.1589 m.

Further, to simulate the wind pressure of 3.5 kPa obtained in wind tunnel tests on full-scale screen prototypes presented in [4] we consider the average velocity $v_m(z^*)$=73.4 m s^{-1}.

The wind force over the generic infill panel is assumed acting along the normal to the panel. Initial configuration coincides with the deployed state after the actuation process. Initial nodal velocities are set to zero. Total time of computation is 250 s.

The time history of the height of the central node of the screen module under wind forces is shown in Figure 3 for a time window of 60 s.

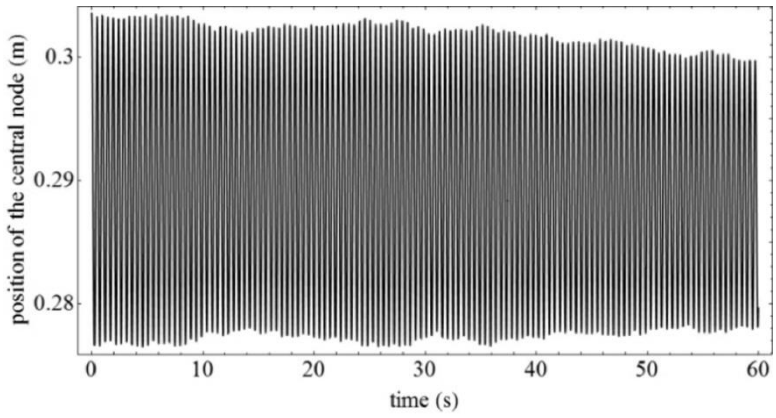

Figure 3. Fluctuation of the height of the central node vs time in the first 60 s of simulation.

It has been observed in [8] that the overall electric energy from WTABS mounted on a façade like that of Al Bahar Towers during actuation is approximately equal to that produced by 233 PV panels and 87 microelolic rooftop turbines with 1 m^2 surface area. The unit cell of the analyzed sunscreen can also produce 2.3 milliwatt hour in presence of wind forces, and such power can be usefully employed to operate microelectronic devices [16].

5. Concluding remarks

The present work has provided comprehensive computational models in matrix and vector forms for the simulation of the dynamics of dynamic solar façades with a tensegrity-based origami architecture. The special ability of such structures to serve as energy harvesters of new generation energy efficient buildings has been diffusely discussed, by considering their actuation motion and wind induced fluctuations. It has been observed that WTABS has good potential for harvesting the energy. Future studies will be focused on the design of modeling of dynamic facades to develop hybrid structures based on natural ventilation and solar shading elements. Energy harvesting researches will be directed towards the use of various piezoelectric elements, such as ceramics, composites, monocrystals and polymers, for the electrical conversion of the energy. The experimental validation of the analyzed sunscreens will be conducted on reduced scale physical models through structural identification procedures.

Acknowledgements
R.M., N.S., and F.F. acknowledge financial support from MIUR under the PRIN 2017 National Grant 'Multiscale Innovative Materials and Structures' (grant number 2017J4EAYB).

References

[1] European Commission, HORIZON 2020 Work Programme 2014-2015, PART 5. II, p 98.
[2] Babilio E, Miranda R and Fraternali F 2019 *Frontiers in Materials* **6**, Article no. 7, pp 48-59.
[3] Armstrong A, Buffoni G, Eames D, James R, Lang L, Lyle J and Xuereb K 2013 *Arup J* **2**, pp 90-95.
[4] Karanouh A and Kerber E 2015 *Journal of Façade Design and Engineering* **3(2)**, pp 185–221.
[5] Balduzzi F, Bianchini A and Ferrari L 2012 *Renewable Energy* **5**, pp.163–174.
[6] Gagliano A, Nocera F, Patania F and Capizzi A. 2013 *Int J Energy Environ Eng* **4** pp 43.
[7] Kosasih B and Tondelli A, 2012 *Procedia Engineering*, *49*, pp 92-98.
[8] Miranda R, Babilio E, Singh N, Santos F and Fraternali F 2020 *Mech Res Commun* **105**, Article no. 103503.
[9] Power Jacks, Rolaram, Electric Linear Actuators. Available at: https:// www.powerjacks.com /perch/resources/brochure/pjlab-rolaram-en-01-1b.pdf.
[10] Skelton R E: 2005 *IUTAM Symposium on Vibration Control of Nonlinear Mechanisms and Structures*, Springer Netherlands pp. 309–318.
[11] Fabbrocino F and Carpentieri G 2017 *Composite Structures* **173**, pp 9–16.
[12] Nagase K and Skelton R E 2014 *Mech Res Commun* **59**, pp 14–25.
[13] Xu X, Li S and Luo Y. 2017 *Mech Res Commun* **84**, pp 1-7.
[14] EN 1991-1-4 (2005): Eurocode 1: Actions on structures, Parts 1-4: General actions. Wind actions.
[15] Santos F, Gonçalves P, Cismaşiu C and Gamboa-Marrufo M 2014 *Proceedings of the Institution of Civil Engineers-Structures and Buildings* **167**(12), pp 743-52.
[16] De Pasquale G 2013 *In Handbook of MEMS for wireless and mobile applications* (Woodhead Publishing) p 345-400.